# Stochastic cellular automata model and Monte Carlo simulations of CD4$^+$ T cell dynamics with a proposed alternative leukapheresis treatment for HIV/AIDS

Monamorn Precharattana [a], Arthorn Nokkeaw [a,b], Wannapong Triampo [a,e,*], Darapond Triampo [a,d], Yongwimon Lenbury [a,c,f]

[a] R&D Group of Biological and Environmental Physics (BIOPHYSICS), Department of Physics, Faculty of Science, Mahidol University, Bangkok, Thailand
[b] Institute for Innovation and Development of Learning Process, Mahidol University, Thailand
[c] Department of Mathematics, Faculty of Science, Mahidol University, Bangkok, Thailand
[d] Department of Chemistry, Center of Excellence for Innovation in Chemistry, Faculty of Science, Mahidol University, Bangkok, Thailand
[e] Center of Excellence for Vector and Vector-Borne Diseases, Mahidol University, Bangkok, Thailand
[f] Center of Excellence in Mathematics, PERDO, Commission on Higher Education, Thailand

## ARTICLE INFO

## ABSTRACT

Acquired Immunodeficiency Syndrome (AIDS) is responsible for millions of deaths worldwide. To date, many drug treatment regimens have been applied to AIDS patients but none has resulted in a successful cure. This is mainly due to the fact that free HIV particles are frequently in mutation, and infected CD4$^+$ T cells normally reside in the lymphoid tissue where they cannot (so far) be eradicated. We present a stochastic cellular automaton (CA) model to computationally study what could be an alternative treatment, namely Leukapheresis (LCAP), to remove HIV infected leukocytes in the lymphoid tissue. We base our investigations on Monte Carlo computer simulations. Our major objective is to investigate how the number of infected CD4$^+$ T cells changes in response to LCAP during the short-time (weeks) and long-time (years) scales of HIV/AIDS progression in an infected individual. To achieve our goal, we analyze the time evolution of the CD4$^+$ T cell population in the lymphoid tissue (i.e., the lymph node) for HIV dynamics in treatment situations with various starting times and frequencies and under a no treatment condition. Our findings suggest that the effectiveness of the treatment depends mainly on the treatment starting time and the frequency of the LCAP. Other factors (e.g., the removal proportion, the treatment duration, and the state of removed cells) that likely influence disease progression are subjects for further investigation.

## 1. Introduction

Human immunodeficiency virus (HIV) infection, which can cause acquired immunodeficiency syndrome (AIDS), has shown a high degree of prevalence in populations all over the world [1]. Since the exact mechanism involved in HIV dynamics and its interaction with the immune system is not well understood, HIV infection is still incurable. The only cost effective treatment is secondary prevention in infected patients by administering several kinds of antiretroviral drugs under a scheme called highly active antiretroviral treatment (HAART), which works to suppress the viral life cycle and prolong the patient's life [2,3]. Although HAART has had a meaningful impact on morbidity and mortality rates [4,5], some patients still suffer because of treatment failure and side effects that vary considerably among individuals and the

particular medicines used in the therapy. Moreover, excessively complicated doses of treatment are a common reason for surrendering and discontinuing HAART [6,7]. Therefore, in order to avoid these clinical problems, an alternative physical strategy is needed.

Apheresis treatment has been studied and used in the treatment of patients with the following conditions: cancer [8–10], autoimmune responses and inflammatory diseases [9,11–15], hepatitis C infection [16,17], and HIV infection [18–21]. Granulocytes/monocytes apheresis in the treatment of HIV infected patients [18–21] suggests that the number of CD4$^+$ T cells increases and is maintained for a period of time after cessation of apheresis courses of treatment, especially in patients who respond to HAART virologically (i.e., their viral load is decreased to a very low level or an undetectable level) [20,21]. In addition, a strong reduction of TNF-α production has been shown [19–21]. However, no evidence of significant change in the viral load has been observed except in one patient reported by Beretta et al. [20] and Lazzarin et al. [18], who was a virological nonresponder who experienced a reduction of HIV plasma viremia due to monocyte/granulocyte removal during the follow-up period. We think that

this lack of change in the viral load is because HIV predominantly grows and infects CD4$^+$ T lymphocytes (CD4$^+$ T cells) [22,23], which generate around 98% of the new virus particles circulating in the blood [24–26]. Therefore, we propose an alternative treatment for HIV/AIDS patients, focusing on lymphocyte removal, namely leukapheresis (LCAP), which is a medical procedure that uses a leukocyte removal filter typically made with polyester fibers to remove leukocyte components via two mechanisms: diameter dependence and leukocyte adherence [27–29].

Previous clinical data of LCAP with Cellsorba FX (Asahi Medical, Tokyo, Japan) [30] suggest that the average percentage of removed cells during a single session of LCAP is nearly 100% for granulocytes and monocytes, and around 60% for lymphocytes—the number of lymphocytes being the key marker of disease progression due to HIV/AIDS. In addition, Sawada et al. [11] report that the level of leukocytes gradually decreases to about 40% of its initial value at the 30 min point of LCAP treatment; however, it gradually rebounds to around 70% at the end of LCAP session, and then further to about 170% during the hours immediately following. This high level of leukocytes then returns to the initial level the following day. This short period overshoot phenomenon was thought to be the result of homeostasis for the number of peripheral leukocytes. It has been hypothesized that since massive amounts of leukocytes are rapidly removed, the overshoot level of the maintenance of leukocytes could not come from the bone marrow but probably from the leukocytes rolling on the vessel or the local inflammatory lesions, including the lymphoid organs. This homeostasis might not only mobilize the leukocytes but also organize the inflammatory cells or the infected cells for entrance into the vessels to adjust the number of leukocytes in the peripheral blood, where these cells again can be removed by the apheresis column (filter). Based on these previous research works and our current understanding of HIV/AIDS, including the advantages of LCAP, we hypothesized that the renewal of circulating lymphocytes by LCAP with an optimal regimen could contribute to a reduction in infected CD4$^+$ T lymphocytes in an HIV infected person.

Several methods [31–39] have been designed to explain the mechanism involved in the interactions between HIV and a patient's immune response, but none of them has completely succeeded. One tool that has been developed to help answer related biological and medical questions is mathematical modeling. Although, the use of ordinary (or partial) differential equations (ODE or PDE) seems to be the favorite way to describe different aspects of the dynamics of virus-host interactions, this method runs into difficulty when a description covering two time scales (short-rang in weeks; long-rang in years) is desired. In addition, it has been suggested that the major source of infection is the lymphoid tissue [40,41] and that a lymph node has a mesh structure which may be represented by a rough surface [42]. Thus, we believe that cellular automata (CA) with carefully selected parameter values can obtain a clearer picture of the effects of HIV infection on the lymphoid tissue.

Cellular automata (CA) [43,44] are discrete mathematical models where we assume that the dynamical system in which we are interested consists of a grid with a discrete variable at each site. The model evolves in discrete time steps according to a definite rule involving local interaction. The advantages of CA include taking into account the local interaction and the two time scales of the HIV infection process. The first CA model regarding the dynamics of HIV and CD4$^+$ T cells was proposed by Santos et al. [45]. This model demonstrates the three phase dynamics of HIV progression, but does not include more details of the virus's participation and replication. Another CA model was designed by Shi et al. [46] for HIV dynamics and included the virus replication cycle and a mechanism for drug therapy.

In our study, we explore a simple CA model associated with the new leukapheresis (LCAP) therapy performed under various schemes. We focus on the changes in CD4$^+$ T cells due to LCAP, varying the treatment procedure initiation and frequency. Our findings suggest that the LCAP regimen could not only prolong an HIV/AIDS patient's life but also be used as an alternative treatment for drug resistant patients or severe cases.

## 2. Model

Our model is based on Shi et al.'s [46] CA model, which describes the evolution of HIV infection under different simulation conditions, such as no treatment, mono or combination therapy, and HAART treatment. Also, some modifications from Santos et al.'s [45] model have been adopted. However, instead of the six states used by Shi et al. [46], we use the five cell states that characterize the life cycle of CD4$^+$ T cells: healthy ($T$), infected stage 1 ($A1$), infected stage 2 ($A2$), latently infected ($A0$), and dead ($D$). The meaning of each of these states is defined as follows:

Healthy ($T$): a cell that stays in an uninfected state and is a target of HIV.
Infected stage 1 ($A1$): a cell that has been recently infected. It carries new virus particles and has not been recognized by the immune cells. Hence, it can infect the healthy ones easily.
Infected stage 2 ($A2$): an infected cell that has been already recognized by the immune cells. This type of cell can thus infect healthy ones only in cases where the concentration is above a certain threshold.
Latently infected ($A0$): a cell that suddenly is in a latent state after it has been infected, yet still can be activated after a long period of dormancy to produce infectious virus particles. Cells in this state cannot transmit an infection to the healthy cells.
Dead ($D$): the state of an infected cell that is killed by the immune response.

In order to investigate two different cases of HIV progression–no treatment and leukapheresis (LCAP) treatment–we describe the life cycle of CD4$^+$ T cells via computer simulations. Our model was performed in MATLAB using the 2-dimensional cellular automata (CA) method. A square shaped lattice of size $L \times L$ grids was used to represent configurations in order to explain the changes in all CD4$^+$ T cell states in a lymph node. Each grid is occupied by a CD4$^+$ T cell in a single state, or it is an unoccupied space, when LCAP is performed.

Since the lymph nodes within the human body are located in several regions and are of different size and because currently there is no estimation of how many runs, how large a lattice size, or what number of immune cells located at each lattice site could represent an entire lymph node, we represent an individual lymph node as a simulation of $100 \times 100$ lattice grids and an average of 1000 runs is interpreted as the dynamics of HIV in an individual patient. The initial configuration (week 1) is depicted as a lymph node randomly contaminated by infected CD4$^+$ T cells—this is referred to as an infected stage 1 ($A1$) cell with a small fraction of $P_{HIV}=0.005$, based on the observation that 1 cell per $10^2$–$10^3$ CD4$^+$ T cells contain viral DNA during primary infection [22]. Then, the states of all cells are updated at each time step, each time step being taken in a unit of one week, corresponding to the rules listed below (see also Fig. 1). In order to maintain the simplicity of the model, we use a time step of one week to compromise between the virus's daily attack on the immune system and the global health of the system which deteriorates in the order of years [47]. When $P_{rem}$ is set to zero, the model simulates the no treatment condition. All parameters chosen (see in Table 1) are based on experimental data; however, some are chosen to obtain quantitative results that agree closely with the typical dynamics of HIV infection (see also Fig. 2).
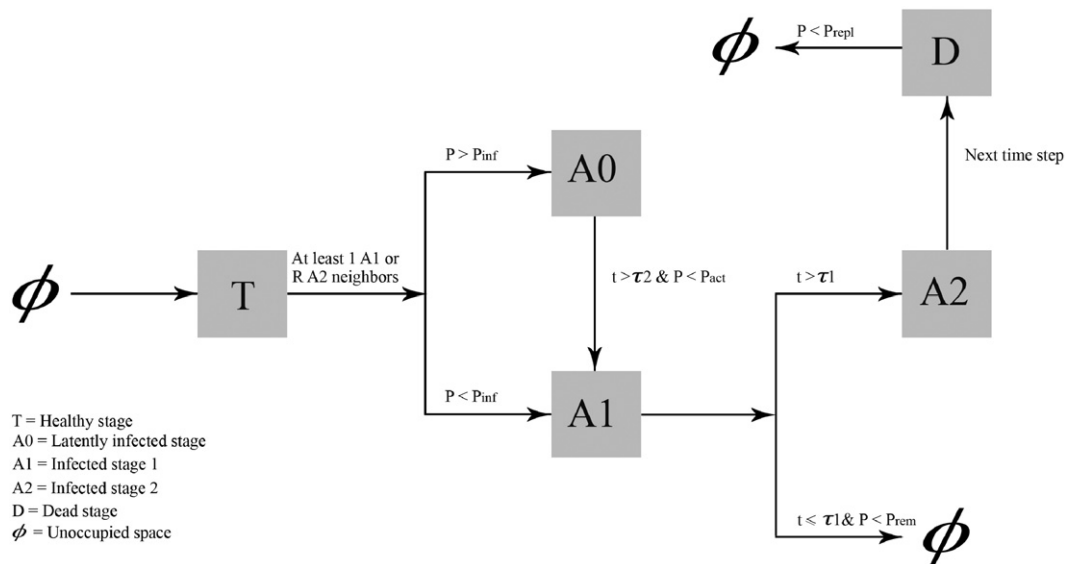
**Fig. 1.** Cell state diagram. A *T* cell becomes an *A*1 cell if it comes in contact with at least one cell of *A*1 or at least *R* cells of *A*2 with the probability $P_{inf}$, or it becomes an *A*0 cell with the probability $1-P_{inf}$. An *A*1 cell is removed by LCAP with the probability $P_{rem}$, or it becomes an *A*2 cell after $\tau 1$ time steps. Then, an *A*2 cell becomes a *D* cell in the following time step, and a *D* cell is replenished by a *T* cell with the probability $P_{repl}$ in the next time step. Moreover, an *A*0 cell becomes an *A*1 cell after $\tau 2$ time steps with the probability $P_{act}$.

**Table 1**
Parameters used.

| Parameter | Description | Value | Source |
|---|---|---|---|
| $L$ | Lattice size, total of cells in the lattice is $L \times L$ | 100 | *Ad hoc* |
| Neighbor cells | The spatial region among the specified cell | 8 | [45] |
| $P_{HIV}$ | Probability or percentage of initial cells contaminated by infected cells | 0.005 | [46] |
| $P_{inf}$ | Probability that a cell becomes actively infected | 0.999 | [46] |
| $P_{rem}$ | LCAP efficacy | 0.9 | *Ad hoc* |
| $P_{act}$ | Probability that an *A*0 cell is activated | 0.0025 | *Ad hoc* |
| $P_{repl}$ | Probability that a *D* cell is replenished by a *T* cell | 0.99 | [45–46] |
| $R$ | Number of *A*2 cells in the neighborhood that can cause the center cell to become infected | 4 | [45–46] |
| $\tau 1$ | Time delay for an *A*1 cell to become an *A*2 cell | 4 | [45–46] |
| $\tau 2$ | Time delay during which an *A*0 cell stays inactive | 30 | [46] |
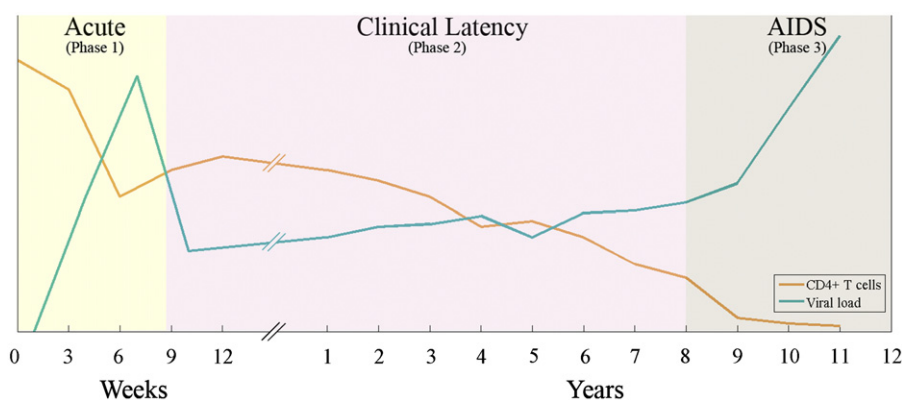


**Fig. 2.** Typical dynamics of HIV. The typical dynamics of HIV divided into three phases and represented in two time scales (weeks and years). The two lines identify the dynamics of CD4$^+$ T cells and the viral load, respectively.

To update each configuration, a cell update is dictated by the state of its neighbors, with the Moore's neighborhood using a neighborhood of range $r=1$ (the number of neighbors is $(2r+1)^2-1$) and the periodic boundary condition.

*Update rule for healthy cells (T)*

*Rule 1.* If a *T* cell has at least one *A*1 cell, or at least *R* infected cells at stage 2 (*A*2), as its neighbors, the *T* cell becomes an *A*1 cell with the probability $P_{inf}$, or it becomes an *A*0 cell with the probability $1-P_{inf}$.

An *A*1 cell is highly capable of spreading HIV to neighboring *T* cells before it is attacked by the immune response. In contrast, an *A*2 cell is at an infected cell stage that has already been attacked by the immune system. It may contaminate the *T* cells before dying if its concentration is above a certain threshold ($R=4$).

After a $T$ cell makes contact with an infected cell, it becomes an infected cell in which its state could be either $A1$ or $A0$.

*Update rule for stage 1 infected cells (A1)*

Rule 2. An $A1$ cell becomes an $A2$ cell after $\tau1$ time steps, or it becomes an unoccupied space ($\phi$) with the probability $P_{rem}$. Otherwise it remains an $A1$ cell.

Once an $A1$ cell is attacked by the immune response, its ability to spread the infection is reduced.

Since HIV has a high frequency rate of mutation and replication, each new infected cell carries a different strain of virus. Hence, we use the time delay $\tau1$ to depict the time that the immune system requires to develop a specific immune response to kill an infected cell. Normally, this parameter may vary from 2 to 6 weeks [45] , but here we let $\tau1=4$.

In addition, for the no treatment condition, $P_{rem}=0$. When the treatment is performed, $P_{rem}=0.9$ which is $A1$ cells are selectively eliminated from the system via LCAP.

*Update rule for stage 2 infected cells (A2)*

Rule 3. An $A2$ cell becomes a $D$ cell in the next time step.

A depletion of infected cells occurs via the immune response.

*Update rule for dead cells (D)*

Rule 4. A $D$ cell is replaced by a $T$ cell with the probability $P_{repl}$ in the next time step. Otherwise it remains unchanged with the probability $1-P_{repl}$.

The replenishment of depleted cells mimics the ability of the immune system to recover from the immuno-suppression generated by infection. Although there is an age-dependent decline in the lymphocyte population and HIV infection leads to a decrease in thymic function [48], we used $P_{repl}=0.99$ to represent the constant and the high probability of immunity replenishment.

*Update rule for latently infected cells (A0)*

Rule 5. After $\tau2$ time steps, an $A0$ cell becomes an $A1$ cell with the probability $P_{act}$, or it stays unchanged.

There is a time delay that an $A0$ cell can be activated above some threshold ($P_{act}=0.0025$) after a long period of dormancy to produce infectious virus particles.

*Update rule for unoccupied space ($\phi$) after leukapheresis treatment*

Rule 6. An unoccupied space ($\phi$) is replaced by a $T$ cell in the next time step.

There is a replacement of $T$ cells to an unoccupied space ($\phi$) by the immune system.

Since LCAP is extracorporal blood circulation therapy (whereas our simulations consider the CD4$^+$ T cell dynamics as occurring in the lymph node), we perform our simulations under the assumption that the infected stage 1 ($A1$) cells, which are selectively removed from the lattice due to LCAP in each step, reflect the dynamics when LCAP is performed, and that all cells can probably flow out from the lymph node through the blood. However, since only $A1$ cells are eliminated from the blood via apheresis, other cells will return to the lymph node at the cessation of the apheresis. Therefore, it should be noted that the number of unoccupied spaces due to LCAP which are expressed in Rule 2 mimics the number of $A1$ cells that are removed from the lymph node, but does not mimic the coordinates of the $A1$ cells which are removed.

## 3. Results and discussion

### 3.1. No treatment

Here, we show our simulation results under the no treatment condition. The results were averaged over 1000 runs or configurations, depending on the accuracy of the data required in order to interpret the dynamics of HIV infection in an individual patient. Generally, the typical dynamics of CD4$^+$ T cells during HIV infection show features as seen in Fig. 3. In addition, although disease
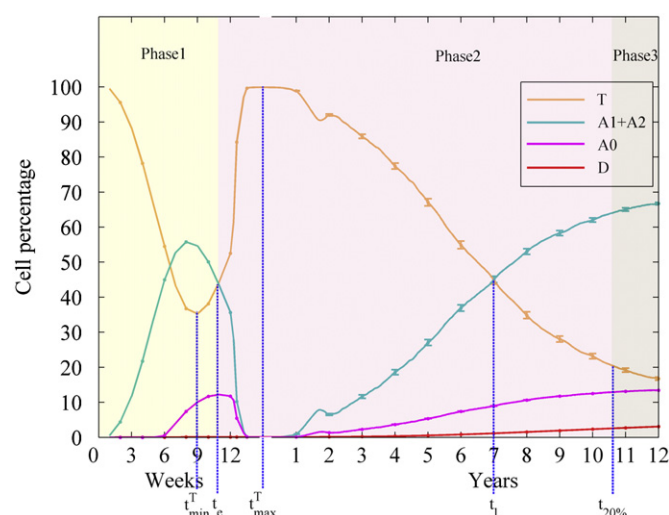


**Fig. 3.** Cell percentage in the natural course of HIV dynamics. The results obtained from our simulations averaged over 1000 runs with $L=100$, $P_{HIV}=0.005$, $P_{inf}=0.999$, $P_{act}=0.0025$, $P_{repl}=0.99$, $R=4$, $\tau1=4$, and $\tau2=30$. The orange line corresponds to healthy cells ($T$); the light blue, infected cells ($A1+A2$); the red, dead cells ($D$); and the violet, latently infected cells ($A0$). The cell dynamics are presented in two time scales (weeks and years) and divided into three phases distinguished by the color shading of the area. The standard error of the mean (SEM) for each cell state is also presented. The small error bars at Phase 1 indicate that its dynamics are insensitive to the initial configuration, in contrast to what is observed in Phase 2 (latency period). The five characteristic times ($t_{min}^T$, $t_e$, $t_{max}^T$, $t_l$, and $t_{20\%}$) are shown. (For interpretation of the references to color in this figure legend, the reader is referred to the web version of this article.)

progression is generally diagnosed via CD4$^+$ T cell count and viral load from a patient's blood, our model simulates the cell dynamics that occur within the lymph node, since it is widely accepted that there is a correlation between the cell population in the blood and the cell population in the lymphoid tissue [23,49]. Therefore, for the sake of our analysis, we divided the data into 3 phases (Phase 1, Phase 2, and Phase 3) relating to the three stages of HIV infection. Each phase is distinguished by colored shading of the area and the labels $t_e$ and $t_{20\%}$. We use $t_e$ and $t_l$ to indicate the time points where the curves of the healthy cells ($T$) and infected cells ($A1+A2$) intersect. $t_{min}^T$ is the time when the number of healthy cells fell to its minimum level in Phase 1, while $t_{max}^T$ is the time when it reaches its maximum in Phase 2. $t_{20\%}$ is used to mark the time when the number of healthy cells is around 20% of the total reservoir.[1] These five characteristic time points were used to mark the temporal transition of CD4$^+$ T cells for the un-treated situation.

The first phase of HIV infection typically stretches from week 1 to about week $t_e$ after the initial infection. This is more or less during the first 11 week period. It was found that there is a rapid increase in the infected cells ($A1+A2$), which peaks at around week 8 ($\sim$56% of the total reservoir), followed by a decline. In contrast, the healthy cells quickly decrease until they reach the minimum, $\sim$35% of the total reservoir ($t_{min}^T$, around week 9); then they rebound later and intersect with the infected cell curve at the early crossing time, $t_e$, when both populations are equal in number ($\sim$44% of the total reservoir), which corresponds to the end of Phase 1.

From the analysis of the spatial configuration randomly generated by the model of an individual simulation, quantitative results like the above are thought to be due to the characteristic transmission of the virus to adjacent cells, where its infectious pattern corresponds to a

---

[1] The total reservoir=the total number of cells (healthy cells+infected cells+latently infected cells+dead cells) in any compartment that serves as a source of the replicating virus.

wave of infected cells propagating in all directions but which then soon clears out from the system. More precisely, such spatial development is due to the dead cells obstructing the newly healthy cells and infected cells at every time step.

Biologically, the primary phase of HIV infection varies from 2 to 6 weeks, during which a dramatic peak in the viral population is invariably associated with a transient reduction in CD4+ T cells [50]. This peak reflects direct infection, ongoing high levels of primary replication, and the disseminated proliferation of HIV, along with activation-induced cell death and host cytotoxic cellular response [50–52]. A decline after the initial peak in the viral population is related to the initiation of an HIV-specific immune response [53] that attempts to eradicate free virus particles and infected cells, and suppresses the viral life cycle after HIV's primary attack.

The second phase of our simulations ranges from week $t_e$ to the week when the number of healthy cells drops to around 20%, which corresponds to approximately week 558 (yr. 10.7). This

phase starts when the healthy cell level rapidly increases after the rebound from the decline that occurs in the first phase—in contrast, the infected cells ($A1+A2$) rapidly decline early on until they reach the minimum ($\sim$0% of the total reservoir). The healthy cells greatly outnumber the infected cells and continue to increase until they reach their maximum, $t_{max}^T$. These phenomena occur over a period of about six months before the number of infected cells increases, and it occurs in conjunction with a slow decrease in the healthy cells until the two curves intersect at the last crossing time, $t_l$, which occurs about week 364 (yr. 7), when the percentages of healthy cells and infected cells are nearly the same ($\sim$45%). After that, the healthy cells drop to a level lower than that of the infected at the following time step.

In our spatial pattern, the slow decrease in healthy cells from $t_{max}^T$ depends on when the latently infected cells ($A0$) are activated. The latently infected cells act like a new source of infection from this time onward, which results in a gradual reduction of healthy cells. The slow dynamics and large deviation
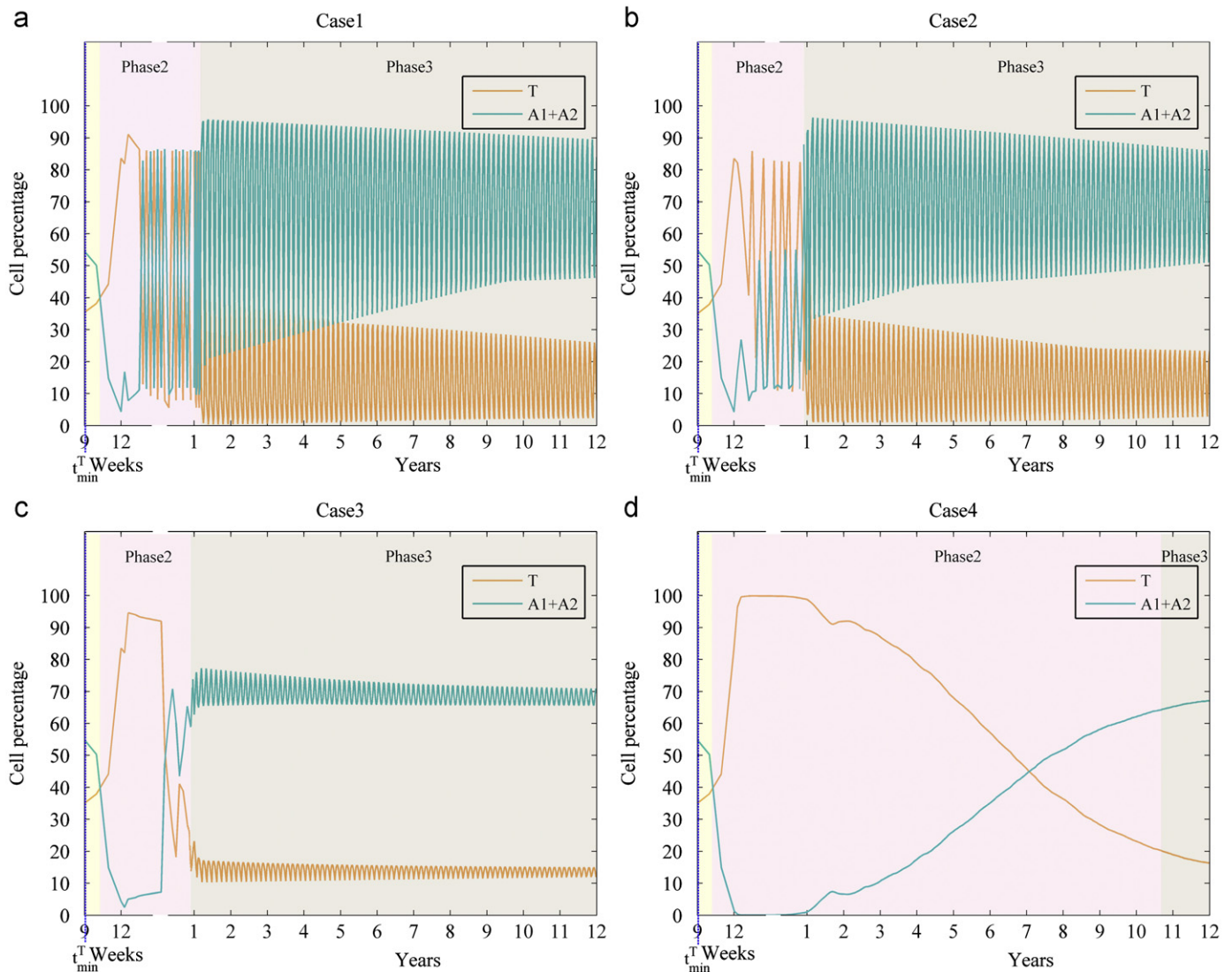


**Fig. 4.** Graph of the percentage of CD4+ T cells with LCAP started at $t_{LCAP1}$ and varying in treatment frequencies. The pictures show the average data of cell dynamics for HIV infection from week $t_{min}^T$ to about year 12. These are the cases where LCAP is started at the second week after the deepest valley of the healthy cells during the first phase of HIV infection ($t_{LCAP1}=t_{min}^T+2$ weeks). The orange line represents the healthy cells ($T$) and the light blue represents the infected cells ($A1+A2$). The results are obtained from 1000 runs; however, the standard error of the mean (SEM) is deserted to avoid crowding. The treatments are performed 13 times with the removal probability $P_{rem}=0.9$. The removal frequencies are varied in 4 cases: (a) Case 1: LCAP is performed every 4 weeks; (b) Case 2: LCAP is performed every 3 weeks; (c) Case 3: LCAP is performed every 2 weeks; and (d) Case 4: LCAP $t_{LCAP1}$ is performed every week. (For interpretation of the references to color in this figure legend, the reader is referred to the web version of this article.)

**Table 2**
Data of healthy cell ($T$) and infected cell ($A1+A2$) dynamics simulated in the no treatment condition and added with the LCAP condition with different frequencies.

| Case | Frequency (every x week(s)) | $t_{min}^T$ week | $P_{min}^T$ % ± SEM ($\sigma^2$) | $t_e$ week | $P_e$ % ± SEM ($\sigma^2$) | $t_{min}^{A1+A2}$ week | $P_{min}^{A1+A2}$ % ± SEM ($\sigma^2$) | $t_{max}^T$ week | $P_{max}^T$ % ± SEM ($\sigma^2$) | $t_l$ week (year) | $P_l$ % ± SEM ($\sigma^2$) | $t_{20\%}$ week (year) | A1+A2 mark period % ± SEM ($\sigma^2$) | T mark period % ± SEM ($\sigma^2$) |
|---|---|---|---|---|---|---|---|---|---|---|---|---|---|---|
| No treatment | | 9 | 35.23 ± 0.14 (19.81) | 11 | 43.63 ± 0.08 (6.94) | 32 | 0.00 ± 0.00 (0.00) | 32 | 99.90 ± 0.00 (0.00) | 364 (7) | 44.96 ± 1.09 (1192.57) | 558 (10.7) | 64.99 ± 0.41 (170.72) | 19.18 ± 0.52 (269.21) |
| 1 | $t_{LCAP1}$ 4 | | | 10.30 | 39.84 ± 0.09 (8.95) | 12 | 4.31 ± 0.02 (0.28) | 16 | 91.14 ± 0.03 (0.74) | 61 (1.2) | 49.07 ± 0.04 (1.22) | 62 (1.2) | 68.26 ± 0.00 (0.00) | 13.57 ± 0.00 (0.02) |
| 2 | $t_{LCAP1}$ 3 | | | 10.30 | 39.73 ± 0.08 (7.76) | 14 | 3.66 ± 0.02 (0.23) | 15 | 92.52 ± 0.03 (0.80) | 49 (0.9) | 49.14 ± 0.04 (1.46) | 50 (1) | 67.74 ± 0.00 (0.02) | 13.81 ± 0.00 (0.00) |
| 3 | $t_{LCAP1}$ 2 | | | 10.30 | 39.72 ± 0.08 (7.84) | 15 | 1.83 ± 0.00 (0.08) | 16 | 94.61 ± 0.02 (0.58) | 39 (0.8) | 49.73 ± 0.19 (34.49) | 42 (0.8) | 68.16 ± 0.00 (0.02) | 13.64 ± 0.00 (0.00) |
| 4 | $t_{LCAP1}$ 1 | | | 10.30 | 39.72 ± 0.09 (8.94) | 23 | 0.00 ± 0.00 (0.00) | 24 | 99.91 ± 0.00 (0.00) | 368 (7.1) | 44.94 ± 1.09 (1188.19) | 558 (10.7) | 65.18 ± 0.40 (160.66) | 18.99 ± 0.50 (253.54) |
| 5 | $t_{LCAP2}$ 4 | | | | | | | | | 130 (2.5) | 46.34 ± 1.25 (1559.45) | 495 (9.5) | 65.72 ± 0.36 (126.69) | 17.61 ± 0.45 (204.29) |
| 6 | $t_{LCAP2}$ 3 | | | | | | | | | 278 (5.3) | 44.87 ± 1.15 (1314.97) | 537 (10.3) | 65.34 ± 0.38 (146.75) | 18.25 ± 0.49 (235.32) |
| 7 | $t_{LCAP2}$ 2 | | | | | | | | | 353 (6.8) | 44.86 ± 1.11 (1235.07) | 549 (10.6) | 65.08 ± 0.42 (176.03) | 18.88 ± 0.53 (277.25) |
| 8 | $t_{LCAP2}$ 1 | | | | | | | | | 378 (7.3) | 44.89 ± 1.09 (1195.27) | 551 (10.6) | 65.26 ± 0.41 (164.12) | 18.89 ± 0.51 (258.08) |
| 9 | $t_{LCAP3}$ 4 | | | | | | | | | | | 417 (8) | 68.90 ± 0.11 (11.06) | 13.84 ± 0.131 (17.18) |
| 10 | $t_{LCAP3}$ 3 | | | | | | | | | | | 405 (7.8) | 68.94 ± 0.12 (14.29) | 14.09 ± 0.15 (22.13) |
| 11 | $t_{LCAP3}$ 2 | | | | | | | | | | | 411 (7.9) | 68.30 ± 0.19 (37.18) | 14.83 ± 0.24 (58.05) |
| 12 | $t_{LCAP3}$ 1 | | | | | | | | | | | 580 (11.2) | 63.66 ± 0.46 (212.08) | 21.33 ± 0.57 (329.79) |

The meaning of the symbols: $t_{min}^T$ = time when the percentage of healthy cells drops to the minimum point during Phase 1. $P_{min}^T$ = the percentage of healthy cells at the minimum point during Phase 1. $t_e$ = the early crossing time (time when the percentage of healthy cells and infected cells intersect at the end point of Phase 1). $P_e$ = the percentage of cells at the early crossing time. $t_{min}^{A1+A2}$ = time when the percentage of infected cells drops to the minimum point during Phase 2. $P_{min}^{A1+A2}$ = the percentage of infected cells at the minimum point during Phase 2. $t_{max}^T$ = time when the percentage of healthy cells reach the maximum point during Phase 2. $P_{max}^T$ = the percentage of healthy cells at the maximum point during Phase 2. $t_l$ = the last crossing time (time when the percentage of healthy cells and infected cells intersect, which occurs during Phase 2). $P_l$ = the percentage of cells at the last crossing time. $t_{20\%}$ = time when the percentage of healthy cells is around 20% of the total cell count. $A1+A2$ = the percentage of infected CD4$^+$ T cells. $T$ = the percentage of healthy CD4$^+$ T cells.

observed in the second phase are related to the emergence of some spatial structures of the infected cells. These growing special structures spread the infection in such a way that they slowly trespass on more and more healthy cells, reducing their number while increasing the number of infected cells.

Clinically, this period lasts approximately one to ten years (or even longer) after the initial infection and is based on the transmission route that determines the initial immune response and viral variability [54]. Although the initiation of the HIV-specific immune response results in a dominating amount of healthy cells during this time, these cells seem incapable of suppressing viral replication completely, since HIV expression persists in the lymph nodes even when viral load is virtually undetectable in the patient's blood. This outcome might well be related to viruses which evolve multiple strategies to evade the immune response [55–57] and establish a state of latency [58]—both of which are known to be the likely causes of the failure to eradicate HIV. The worsening of the immune system is manifested by the reduction of CD4$^+$ T cells.

On comparing our results to the clinical experiment, our quantitative results show the healthy cells ($T$) rebounding to the highest level ($t_{max}^T$) and the infected cells ($A1+A2$) transiently increasing, while the results obtained from the clinical experiment show CD4$^+$ T cells rebounding toward baseline levels; however, they still remain lower than those seen prior to infection, and the viral load completely goes down to an undetectable level that generally corresponds to a steady state.

The third phase of HIV infection begins at $t_{20\%}$ (i.e., about week 558 or year 10.7). The healthy cells continually drop to a level lower than 20% until year 12, as is typical in the normal course of \HIV infection. We mark the last 100 weeks, week 525 to week 624, as the period to distinguish the reduction of infected CD4$^+$ T cells. This period of the last 100 weeks is known as the *mark period*,[2] where the healthy cells ($T$) and the infected cells ($A1+A2$) are approximately 19.18% and 64.99% of the total reservoir, respectively.

Clinically, the inevitable outcome of the progressive deterioration of the immune system that occurs in most HIV patients in this period is a clinically apparent disease or acquired immunodeficiency syndrome (AIDS), which includes severe or persistent signs of illness or an opportunistic infection or neoplasm. Normally, doctors define this stage as occurring when the CD4$^+$ T cell count drops to lower than 200 cells per μL, which is approximately 20% of the normal value in a healthy person. Subsequently, the level approaches zero, and death usually occurs within two years. What we could reproduce in our model was healthy cell dynamics decreasing slightly to less than 20% toward a steady state.

We turn next to CD4$^+$ T cell dynamics under various LCAP treatment schemes.

### 3.2. With LCAP treatment

We wish to explore whether or not LCAP helps patients and, if so, under what treatment schemes and to what extent, since changes in cell population depend on several parameters, including LCAP starting time, LCAP frequency, cell removal proportion size, and treatment duration.

In this section, we present simulation results on CD4$^+$ T cells with LCAP treatment under various frequency schemes for each LCAP starting time. Each starting time corresponds to a time that is about a few weeks after the characteristic time $t_{min}^T$, $t_{max}^T$, or $t_l$. The

---

² We mark this period for investigating the reduction of infected cells ($A1+A2$) in a normal case versus one where the LCAP regime has been added. To find the average dynamics in this period, we first consider the convergence of cell dynamics during weeks 525–624 of an individual run and then average the convergence of the total runs to be the mark period.

characteristic times are taken from an average of 1000 runs, which represents an individual patient. The algorithms are as follows.

○ Starting LCAP at $t_{LCAP1}$. For each individual run, the first LCAP session is started at the second week after the deepest valley of healthy cells is observed, $t_{min}^T$, during the first phase of HIV infection ($t_{LCAP1}=t_{min}^T+2$ weeks). We apply LCAP at the second week after the characteristic time in which the trend of healthy cell dynamics has certainly changed, in order to see what is going to happen if the $A1$ cells are removed while the number of healthy cells is rising.

○ Starting LCAP at $t_{LCAP2}$. For each individual run, the first LCAP session is started at the second week after the healthy cells reach their maximum level, $t_{min}^T$, during the second phase of HIV infection ($t_{LCAP2}=t_{max}^T+2$ weeks) to investigate the effect of apheresis when the $A1$ cells are removed while the number of healthy cells is gradually dropping but still is larger than that of the infected.

○ Starting LCAP at $t_{LCAP3}$. For each individual run, the first LCAP session is started at the second week after the last crossing time point, $t_l$, between the healthy cell and infected cell curves ($t_{LCAP3}=t_l+2$ weeks) to investigate the effect of apheresis when the $A1$ cells are removed while the number of healthy
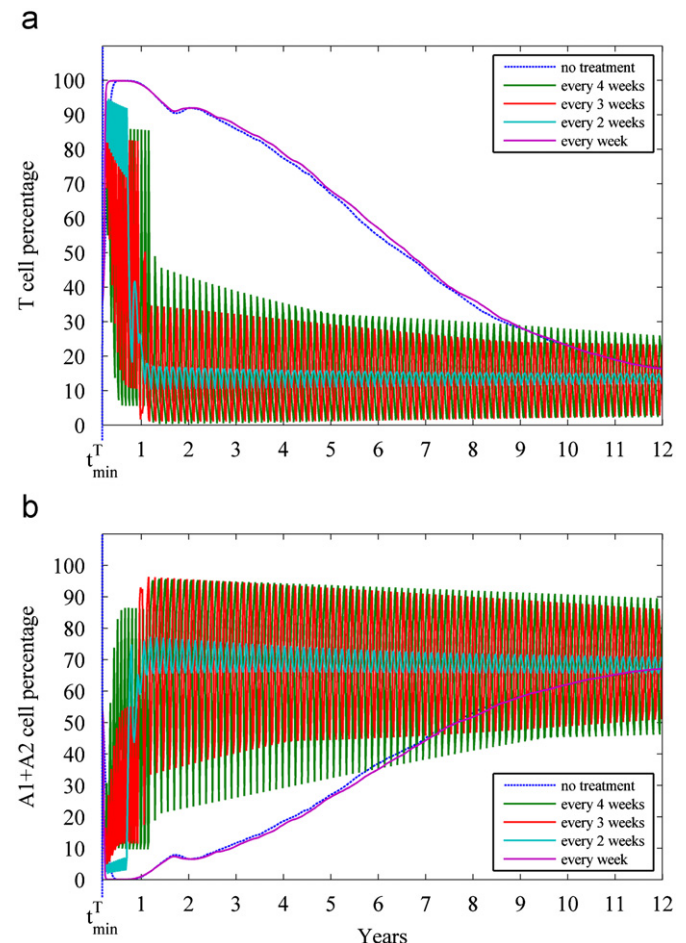


**Fig. 5.** Comparison of cell dynamics at different frequencies with LCAP started at $t_{LCAP1}$. The pictures show the cell dynamics from week $t_{min}^T$ to about year 12, where picture (a) shows the percentage of healthy cell dynamics ($T$) and picture (b) shows the percentage of infected cell dynamics ($A1+A2$). The blue dashed line corresponds to the cell dynamics with no treatment. The green line corresponds to the cell dynamics when LCAP is performed once every 4 weeks, the red line once every 3 weeks, the light blue line once every 2 weeks, and the violet line once every week. (For interpretation of the references to color in this figure legend, the reader is referred to the web version of this article.)

cells is gradually dropping and when their number is less than that of the infected.

We assume that the LCAP filter is developed to the proficiency where the state of the cell is distinguishable, and we investigate the frequencies of treatment by removing the infected cells at stage 1 ($A1$), since the $A1$ cells are most efficient at infecting healthy cells. The apheresis is done every 4 weeks, every 3 weeks, every 2 weeks, and every week. Under the assumption that LCAP is highly efficient, we use the *removal proportion*, $P_{rem}$, of 0.9, and the total number of treatments is chosen to be 13 in order to limit the treatment duration to approximately 3 months for every one week LCAP condition and to approximately 1 year for every 4 weeks LCAP condition.

Since the dynamics of the latently infected state and the dead state in our simulations are found not to change significantly when LCAP is performed, we thus deliver and describe our results only in relation to healthy cell dynamics ($T$) and infected cell dynamics ($A1+A2$).

### 3.2.1. Cases where cell removal is started at $t_{LCAP1}$

$A1$ cell removal is performed at a frequency of every 4, 3, 2, and 1 week(s), corresponding to cases 1, 2, 3, and 4, respectively (see Fig. 4a–d). We find that the early crossing time $t_e$ occurs around day 72 (week 10.3), when both the healthy cells and the infected cells ($A1+A2$) are around 39.75% (in the range 39.72–39.84%. See also Fig. 4 and Table 2), and before the healthy cells reach their maximum: $t_{max}^T \sim 91.14\%$, $\sim 92.52\%$, $\sim 94.61\%$, and $\sim 99.91\%$ around weeks 16, 15, 16, and 24 for cases 1, 2, 3, and 4, respectively. At the last crossing time, $t_l$, both the healthy cells and the infected cells are in the 44.94–49.73% range, with an average of about 48.22%. This $t_l$ corresponds approximately to weeks 61, 49, 39, and 368 (yr. 7) for cases 1, 2, 3, and 4, respectively. The third phase of HIV infection (when the level of healthy cells is just below 20% at $t_{20\%}$) occurs
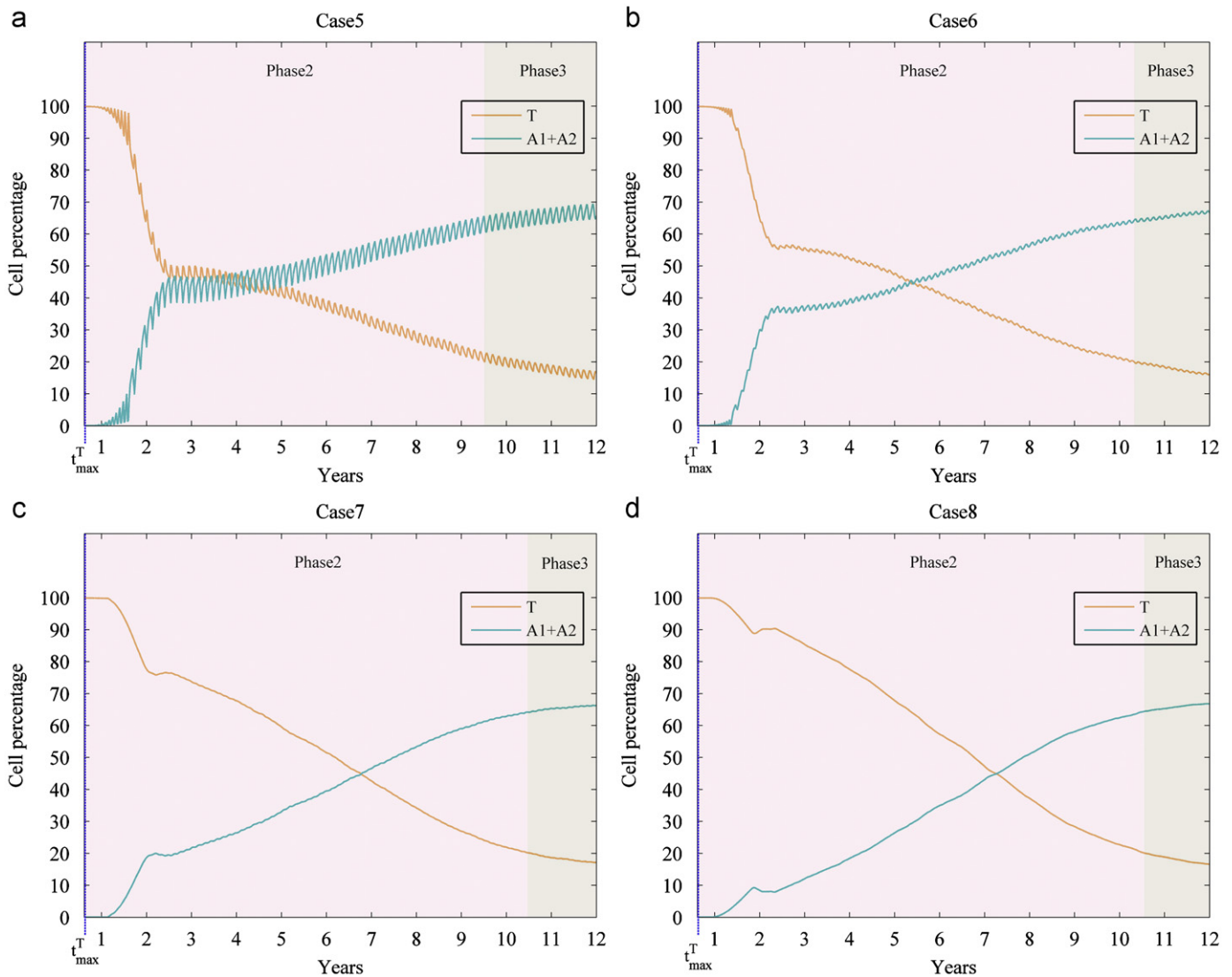


**Fig. 6.** Graph of the percentage of CD4$^+$ T cells with LCAP started at $t_{LCAP2}$ and varying in treatment frequencies. The pictures show the average data of cell dynamics for HIV infection from week $t_{max}^T$ to about year 12. These are the cases where LCAP is started at the second week after the maximum point of healthy cells during the second phase of HIV infection ($t_{LCAP2} = t_{max}^T + 2$ weeks). The orange line represents the healthy cells ($T$) and the light blue represents the infected cells ($A1+A2$). The results are obtained from 1000 runs; however the standard error of the mean (SEM) is deserted to avoid crowding. The treatments are performed for 13 times with the removal probability $P_{rem} = 0.9$. The removal frequencies are varied in 4 cases: (a) Case 5: LCAP is performed every 4 weeks; (b) Case 6: LCAP is performed every 3 weeks; (c) Case 7: LCAP is performed every 2 weeks; and (d) Case 8: LCAP is performed every week. (For interpretation of the references to color in this figure legend, the reader is referred to the web version of this article.)

around weeks 62, 50, 42, and 558 (yr. 10.7) for cases 1, 2, 3, and 4, respectively—when the level of healthy cells is approximately 15% of the total reservoir (in the range 13.57–18.99%). In contrast, the corresponding level of infected cells rises rapidly to approximately 67.33% (in the range 65.18–68.26%). The healthy and infected cells both vary in a cyclic fashion.

These results suggest that the course of HIV infection combined with LCAP started at $t_{LCAP1}$ under relatively low frequency conditions (case 1, case 2, and case 3) exhibits more rapid dynamics (for changes in cell population, see Fig. 5a and b) than that which is observed during the natural course of HIV infection without LCAP. In addition, it is clearly seen that the level of healthy cells reaches its maximum sooner and its peaks are lower. Moreover, the third phase of infection is reached suddenly (about 1 year) after the treatment has ceased. When we look closely at the cyclic behavior of cell dynamics during the treatment, it varies greatly from case to case. The period and the amplitude of these cycles depend on the removal frequency. A lower frequency—for instance, aphersis treatment every 4 weeks—corresponds to higher amplitude (see e.g., Fig. 5a and b). These amplitudes are related to the losses and gains of the $A1$ cells after each LCAP session. This cyclic behavior is comparable to that of the waste product levels found in each cessation of hemodialysis treatment [59]. However, the cyclic pattern turns into a vibration with a period of 7 time steps after the treatment ceases, decaying over time. This period relates to the number of time steps in one life cycle simulation of the $CD4^+$ T cells after infection, as shown in Fig. 1.

In contrast, the dynamics under a high removal frequency, case 4 (see Fig. 4d), are more similar to that of the natural course of HIV infection. Their mark points are not changed significantly and differ only in that the healthy cells' maximum point, $t^T_{min}$, is reached earlier—as is seen in Fig. 5a (violet line). These differences in $t^T_{min}$ might result from the early continuous reduction of the $A1$ cells, which are replenished by healthy cells every week during the LCAP. The LCAP, which is performed from around week 11 to week 23 (~3 months), lasts over a very short period compared to the course of infection; consequently, the treatment regime ceases before the activation of the latently infected cells ($\tau2=30$). Thus, it seems that the short perturbation period in the early phase of the dynamics will not produce a significant change in the whole scheme of the system. However, it is noted that stochastic variations could cause a change in the infected cells between week 10 and week 11, which would result in an incident of $t_e$ about week 10.3, instead of week 11.

In summary, the course of HIV infection with LCAP under the high frequency regime where $A1$ cells are removed every week might translate to a prolonged quality of life for patients if they receive treatment for a suitable duration.

### 3.2.2. Cases where cell removal is started at $t_{LCAP2}$

For the cases (case 5–case 8) where cell removal is started at $t_{LCAP2}$ (see Fig. 6a–d), since the procedure is performed around the second week after the progression reaches the healthy cells' maximum point, $t^T_{max}$, (around week 32), the removal frequency does not affect the early crossing time $t_e$. We thus investigated the cell dynamics at $t_{LCAP2}$ and found that LCAP effects the last crossing time $t_l$, which appears when the levels of healthy cells and infected cells ($A1+A2$) are equal—at around 45.24% of the total reservoir (in the range 44.86%-46.34%. See also Table 2). This occurs at about weeks 130 (yr. 2.5), 278 (yr. 5.3), 353 (yr. 6.8), and 378 (yr. 7.3) for cases 5, 6, 7, and 8, respectively—which is before the third phase of HIV infection is reached around weeks 495 (yr. 9.5), 537 (yr. 10.3), 549 (yr. 10.6), and 551 (yr. 10.6) for cases 5, 6, 7, and 8, respectively. At the third phase, the number of healthy cells is nearly 18.41% of the total reservoir (in the range

17.61–18.89%), while that of the infected cells is around 65.35% of the total reservoir (in the range 65.08–65.72%).

These findings suggest that the initial cell removal at $t_{LCAP2}$ at low frequencies (as in cases 5–7) might affect the time consumption in each phase of the cell dynamics, as is previously seen under the low frequency conditions for $t_{LCAP1}$. Cyclic patterns of cell dynamics are also seen in Fig. 6a and b, where the rush of dynamics to the last crossing over time is observed; however the third phase of infection for every case at the low frequency condition occurs at nearly the base line (no treatment case) (see also Fig. 7a and b). In contrast with the high frequency case (case 8), the dynamics are rather the same as the base line but slower in cell dynamics (see Fig. 7a and b: violent line). This is because we use a high frequency treatment at $t_{LCAP2}$. Hence, the healthy cells remain at the maximum level during the treatment. And when the treatment ceases, after the time when the first latently infected cells ($A0$) are activated, the number of healthy cells continuously drops to the third phase with the same pattern as that observed in the no treatment case.

In summary, the scenario of removing cells every week at the $t_{LCAP2}$ condition might benefit patients by prolonging their lives if we extend the treatment duration.
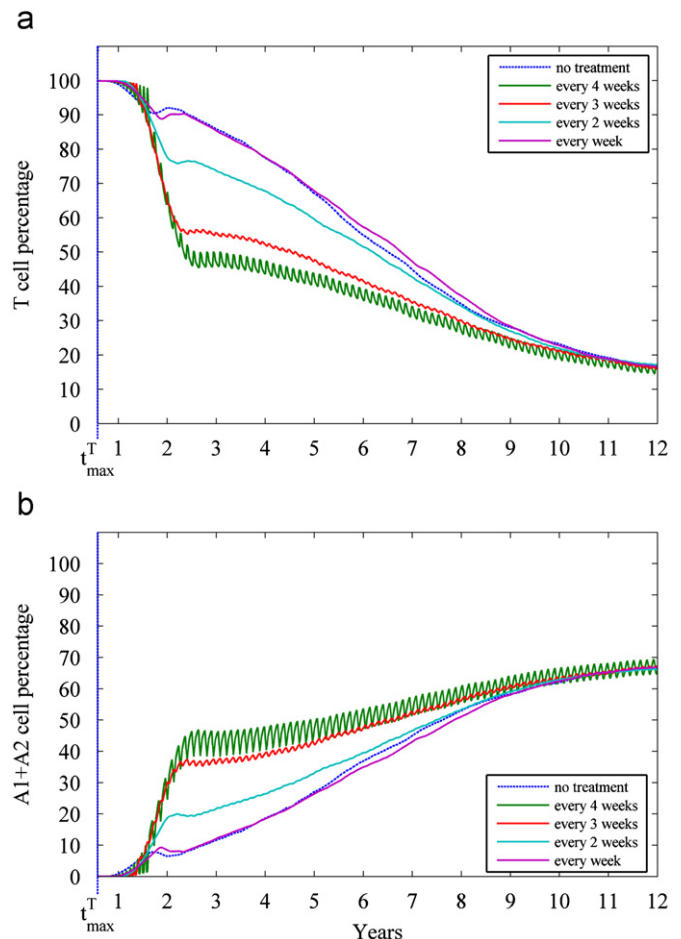


**Fig. 7.** Comparison of cell dynamics at different frequencies with LCAP started at $t_{LCAP2}$. The pictures show the cell dynamics from week $t^T_{max}$ to about year 12, where picture (a) shows the percentage of healthy cell dynamics ($T$) and picture (b) shows the percentage of infected cell dynamics ($A1+A2$). The blue dashed line corresponds to the cell dynamics with no treatment. The green line, the red line, the light blue line, and the violet line correspond to the cell dynamics for LCAP performed once every 4, 3 2, and 1 week(s), respectively. (For interpretation of the references to color in this figure legend, the reader is referred to the web version of this article.)

### 3.2.3. Cases where cell removal is started at $t_{LCAP3}$

We now consider cases 9, 10, 11, and 12 for cell removal every 4, 3, 2, and 1 week(s), respectively (see Fig. 8a–d). For the LCAP starting at $t_{LCAP3}$, which is after the last crossing time $t_l$ (around week 2), the four characteristic times $t_{min}^T, t_e, t_{max}^T$, and $t_l$ regularly occur around the week that is very close to the baseline data of the cell dynamics in the no treatment case. $t_{LCAP3}$ marks the occurrence of the third phase of infection, $t_{20\%}$, which is around weeks 417 (yr. 8), 405 (yr. 7.8), 411 (yr. 7.9), and 580 (yr. 11.2) for cases 9, 10, 11, and 12, respectively (see also Table 2). The corresponding number of healthy cells is, on average, 16.02% of the total reservoir (in the range 13.84–21.33%). The number of infected cells ($A1+A2$) in these cases is, on average, 67.45% of the total reservoir (in the range 63.66–68.94%). Comparisons among the results of the low frequency cases demonstrate that only case 11 (cell removal every 2 weeks) affects the cyclic pattern of the healthy cells' increment above the baseline and the infected cells' degradation under the baseline during the course of treatment (see Fig. 9a and b). This suggests that removing every 2 weeks

(case 11) might benefit a patient by prolonging the patient's life during continuation of LCAP. In addition, we find that removing at high frequency (case 12) produces an increase in the number of healthy cells during the treatment until the population nearly peaks (~99% of the total reservoir), which occurs at the same time that the number of infected cells almost reaches the bottom level (~0% of the total reservoir) (see Fig. 8d).

After the treatment ceases, there is a lengthy decrease in the healthy cells associated with a slow increase in the infected cells until the boundary time is crossed again. This time point is at approximately week 463 (yr. 8.9) and represents the last crossing time of the infection after treatment. In our opinion, the cell dynamics pattern of case 12 seems to repeat the normal pattern of HIV infection after treatment. However, we would like to note that although in our model the apheresis for case 12 helps the healthy cells to recover and return to the point of the previous maximum, the apheresis under this condition only helps in reducing the number of actively infected cells; it does not remove the latently infected cells ($A0$). Hence, after we cease the treatment, both the healthy cell and infected cell
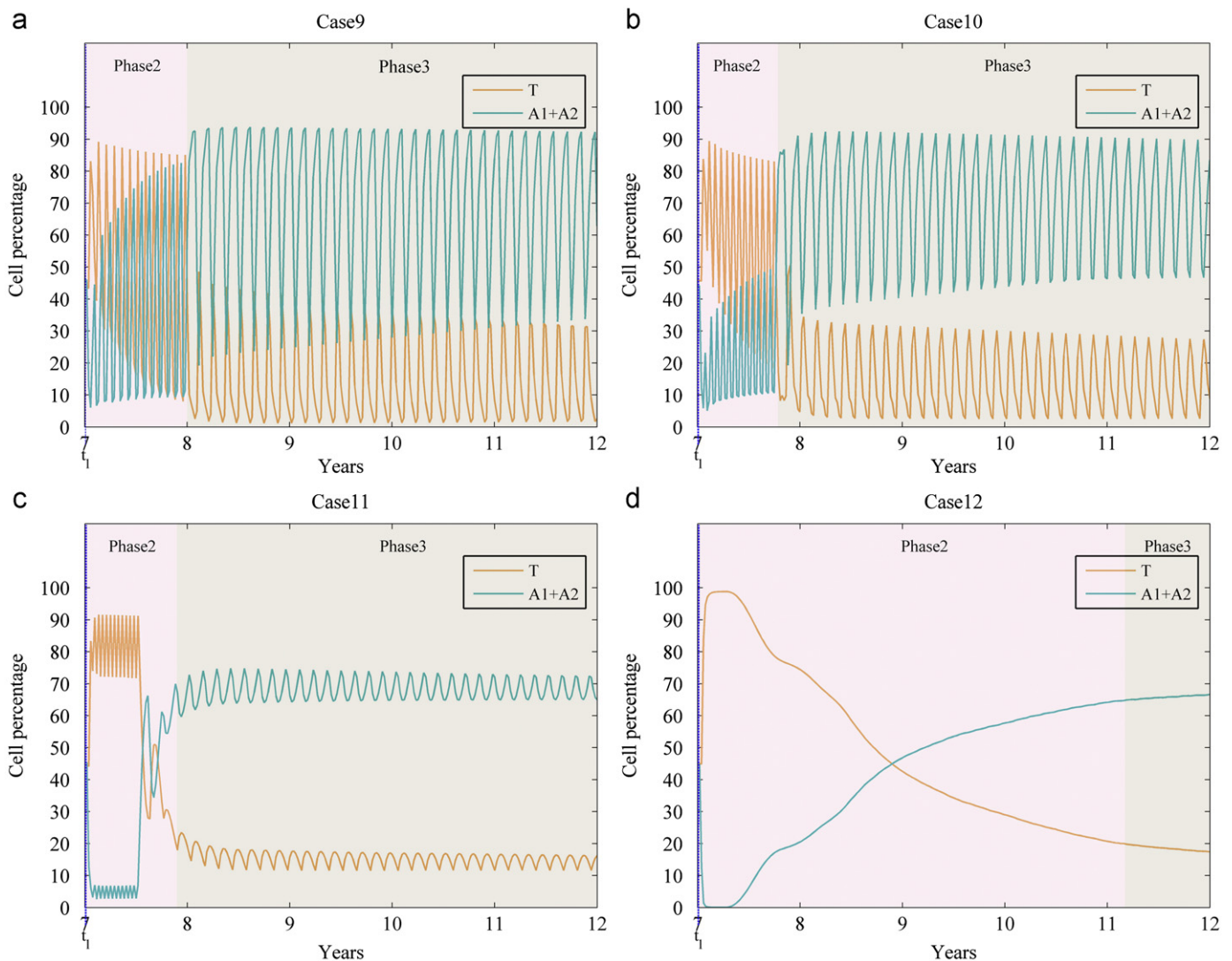


**Fig. 8.** Graph of the percentage of CD4$^+$ T cells with LCAP started at $t_{LCAP3}$ and varying in treatment frequencies. The pictures show the average data of cell dynamics for HIV infection from year $t_l$ to about year 12. These are the cases where LCAP is started at the second week after the last cross over time between the healthy cells and the infected cell curves during the second phase of HIV infection ($t_{LCAP3} = t_l + 2$ weeks). The orange line represents the healthy cells ($T$) and the light blue represents the infected cells ($A1+A2$). The results are obtained from 1000 runs; however the standard error of the mean (SEM) is deserted to avoid crowding. The treatments are performed 13 times with the removal probability $P_{rem} = 0.9$. The removal frequency is varied in 4 cases: (a) Case 9: LCAP is performed every 4 weeks; (b) Case 10: LCAP is performed every 3 weeks; (c) Case 11: LCAP is performed every 2 weeks; and (d) Case 12: LCAP is performed every week. (For interpretation of the references to color in this figure legend, the reader is referred to the web version of this article.)
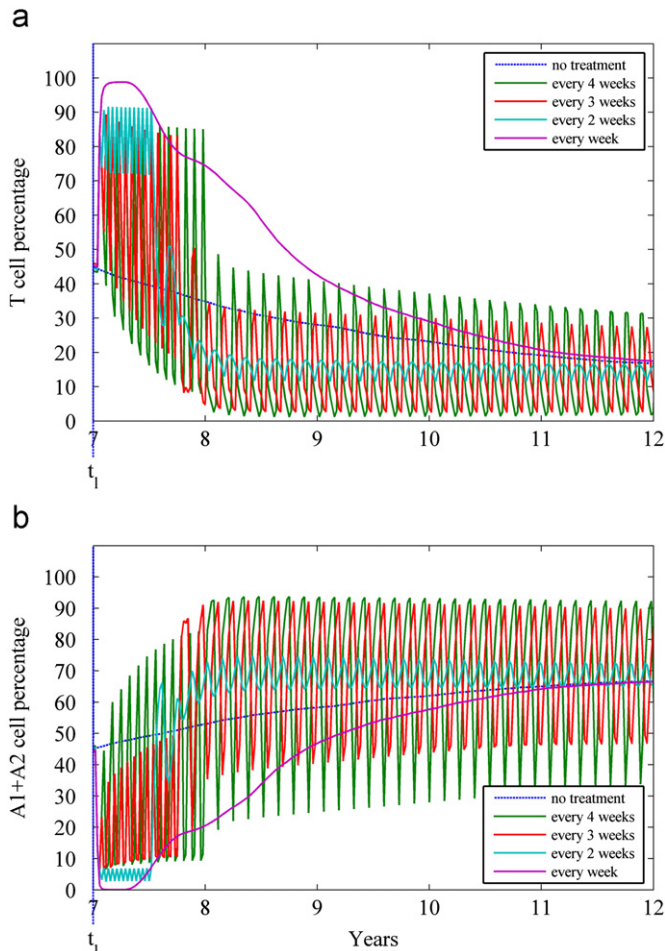
Fig. 9. Comparison of cell dynamics at different frequencies with LCAP started at $t_{LCAP3}$. The pictures show the cell dynamics from year $t_l$ to about year 12, where picture (a) shows the percentage of healthy cell dynamics ($T$), and picture (b) shows the percentage of infected cell dynamics ($A1+A2$). The blue dashed line corresponds to the cell dynamics with no treatment. The green line, the red line, the light blue line, and the violet line correspond to the cell dynamics for LCAP performed once every 4, 3 2, 1 week(s), respectively. (For interpretation of the references to color in this figure legend, the reader is referred to the web version of this article.)

dynamics are faster than that which occurs in the natural course of infection due to the accumulation of $A0$ cells over time. The quantitative results also suggest that the apheresis treatment could only help in reducing the number of infected cells and recovering the healthy ones. It could not help the lymphoid tissue (e. g., lymph node) already damaged by HIV infection become healthy again.

In summary, removing cells once every 2 weeks (case 11) and removing them once every week (case 12) at $t_{LCAP3}$ might improve and prolong the patient's life, but in case 11 only when the patient was undergoing the apheresis. For case 12, this remedy works as if we have refreshed the reservoir to the point where there are plentiful healthy cells, along with a few latently infected cells remaining after the treatment ceases. Subsequently, the dynamics will relax to the baseline pattern after the first latently infected cell is activated.

## 4. Concluding remarks

According to our model algorithm and the controlled parameters, it appears that under certain LCAP treatment conditions, infected CD4$^+$ T cell populations ($A1+A2$) can be reduced. Our

findings indicate that the course where LCAP is started at $t_{LCAP3}$ and cells are removed once every week (case 12) might be the most effective scheme toward prolonging a patient's life. When LCAP is started at $t_{LCAP3}$ (while the level of infected CD4$^+$ T cells continually increases), the $A1$ cell removal per LCAP session is relatively high compared to starting the treatment at either $t_{LCAP1}$ or $t_{LCAP2}$. These results are supported by recent research works [60–65], which describe the benefits of greater frequency in hemodialysis treatments. Hence, we suggest that it might be suitable to increase LCAP frequency to more than once a week. This adjustment would provide the immune system with a better chance to fight the existing virus during the critical third phase of HIV/AIDS. Therefore, it might be reasonable to adopt this LCAP protocol as an additional treatment, with fewer side effects, for HIV/AIDS when there is resistance to current drug therapies. Still, this is an arguable proposition that needs to be experimentally explored in further research. Our investigation still leaves many questions in need of answers. For example, what would happen if we change the removal proportion? Can the long treatment duration break the infected cells' set point or just prolong the patient's life? We hope that our results will inspire others in the field to investigate such questions.

## Conflict of interest statement

None declared.

## Acknowledgments

## References

[1] W.H.O. Unaids, A. E. update. Geneva: UNAIDS, WHO (2007).
[2] D.B. Clifford, C. Yiannoutsos, M. Glicksman, D.M. Simpson, E.J. Singer, P.J. Piliero, C.M. Marra, G.S. Francis, J.C. McArthur, K.L. Tyler, A.C. Tselis, N.E. Hyslop, HAART improves prognosis in HIV-associated progressive multi-focal leukoencephalopathy, Neurology 52 (1999) 623–625.
[3] H. Albrecht, C. Hoffmann, O. Degen, A. Stoehr, A. Plettenberg, T. Mertensk tter, C. Eggers, H.J. Stellbrink, Highly active antiretroviral therapy significantly improves the prognosis of patients with HIV-associated progressive multi-focal leukoencephalopathy, AIDS 12 (1998) 1149–1154.
[4] E.L. Murphy, A.C. Collier, L.A. Kalish, S.F. Assmann, M.F. Para, T.P. Flanigan, P.N. Kumar, L. Mintz, F.R. Wallach, G.J. Nemo, Highly active antiretroviral therapy decreases mortality and morbidity in patients with advanced HIV disease, Ann. Intern. Med. 135 (2001) 17–26.
[5] F.J. Palella, K.M. Delaney, A.C. Moorman, M.O. Loveless, J. Fuhrer, G.A. Satten, D.J. Aschman, S.D. Holmberg, Declining morbidity and mortality among patients with advanced human immunodeficiency virus infection, N. Engl. J. Med. 338 (1998) 853–860.
[6] S. Bassetti, M. Battegay, H. Furrer, M. Rickenbach, M. Flepp, L. Kaiser, A. Telenti, P.L. Vernazza, E. Bernasconi, P. Sudre, Why is highly active antiretroviral therapy (HAART) not prescribed or discontinued? JAIDS—J. Acq. Imm. Def. 21 (1999) 114–119.
[7] L. Maisels, J. Steinberg, C. Tobias, An investigation of why eligible patients do not receive HAART, Aids Patient Care St. 15 (2001) 185–191.
[8] T. Tabuchi, H. Ubukata, A.R. Saniabadi, T. Soma, Granulocyte apheresis as a possible new approach in cancer therapy: a pilot study involving two cases, Cancer Detect. Prev. 23 (1999) 417–421.

[9] M. Yonekawa, A. Kawamura, T. Komai, T. Agishi, M. Adachi, Extracorporeal granulocytapheresis for cancer and rheumatoid arthritis, Transfus. Sci. 17 (1996) 463–472.

[10] T. Tabuchi, H. Ubukata, S. Sato, I. Nakata, Y. Goto, Y. Watanabe, T. Hashimoto, T. Mizuta, M. Adachi, T. Soma, Granulocytapheresis as a possible cancer treatment, Ther. Apher. 4 (2001) 155–160.

[11] K. Sawada, K. Ohnishi, T. Kosaka, S. Chikano, Y. Yokota, A. Egashira, H. Izawa, M. Yamamura, K. Amano, M. Satomi, T. Shimoyama, Leukocytapheresis with leukocyte removal filter as new therapy for ulcerative colitis, Ther. Apher. Dial. 1 (1997) 207–211.

[12] W.J. Sandborn, Preliminary data on the use of apheresis in inflammatory bowel disease, Inflamm. Bowel Dis. 12 (2006) S15–S21.

[13] T. Furuta, O. Hotta, N. Yusa, I. Horigome, S. Chiba, Y. Taguma, Lymphocytapheresis to treat rapidly progressive glomerulonephritis: a randomised comparison with steroid-pulse treatment, Lancet 352 (1998) 203–204.

[14] T. Matsui, T. Nishimura, H. Matake, T. Ohta, T. Sakurai, T. Yao, Granulocytapheresis for Crohn's disease: a report on seven refractory patients, Am. J. Gastroenterol. 98 (2003) 511–512.

[15] H. Miyamoto, T. Okahisa, H. Iwaki, M. Murata, S. Ito, Y. Nitta, M. Akutagawa, Y. Kinouchi, Y. Ohnishi, J. Oto, M. Nishimura, Influence of leukocytapheresis therapy for ulcerative colitis on anemia and hemodynamics, Ther. Apher. Dial. 11 (2007) 16–21.

[16] K. Sawada, K. Ohnishi, K. Fukunaga, T. Shimoyama, A new treatment for HCV-ulcerative colitis comorbidity intolerant to INF-α, Am. J. Gastroenterol. 98 (2004) 228–229.

[17] H.M. Diepolder, N. Kashiwagi, G. Teuber, A. Ulsenheimer, M. Franz, T. Yokoyama, R. Zachoval, Leucoytapheresis with Adacolumn (R) enhances HCV-specific proliferative responses in patients infected with hepatitis C virus genotype 1, J. Med. Virol. 77 (2005) 209–215.

[18] A. Lazzarin, M. Clerici, H. Hasson, L. Fumagalli, P. Ferrante, A.R. Saniabadi, M. Adachi, A. Beretta, Immunovirological improvement in partially HAART responder HIV-infected patients by monocyte adsorption apheresis, J. Clin. Apheresis 16 (2001) 35–36.

[19] A. Beretta, M. Clerici, H. Hasson, L. Fumagalli, D. Trabattoni, F. Lillo, P. Ferrante, A.R. Saniabadi, M. Adachi, A. Lazzarin, Ex-vivo purging of circulating monocytes results in immunovirologic improvement in partially HAART responder HIV-infected patients, J. Biol. Regul. Homeost. Agents 14 (2000) 27–31.

[20] A. Beretta, H. Hasson, A. Samiabadi, M. Alfano, D. Trabattoni, F. Lillo, P. Ferrante, M. Clerici, A. Lazzarin, Selective granulocyte/monocyte apheresis in the treatment of HIV-infected patients: short–term and long-term effects on immunological and virological parameters, Perfusion 17 (2002) 47–51.

[21] H. Hasson, A. Saniabadi, M. Alfano, D. Trabattoni, P. Ferrante, F. Lillo, M. Clerici, A. Lazzarin, A. Beretta, Granulocyte/monocyte apheresis induces sustained increases in CD4 T cells in HIV-1 infected patients with poor CD4 T cell restoration after suppression of viral replication by HAART, J. Biol. Regul. Homeost. Agents 16 (2002) 58–63.

[22] S.M. Schnittman, M.C. Psallidopoulos, H.C. Lane, L. Thompson, M. Baseler, F. Massari, C.H. Fox, N.P. Salzman, A.S. Fauci, The reservoir for HIV-1 in human peripheral blood is a T cell that maintains expression of CD4, Science 245 (1989) 305–308.

[23] T. Schacker, S. Little, E. Connick, K. Gebhard, Z. Zhang, J. Krieger, J. Pryor, D. Havlir, J. Wong, R.T. Schooley, D. Richman, L. Corey, A.T. Haase, Productive infection of T cells in lymphoid tissues during primary and early human immunodeficiency virus infection, J. Infect. Dis. 183 (2001) 555–562.

[24] C. Briones, E. Domingo, C. Molina-París, Memory in retroviral quasispecies: experimental evidence and theoretical model for human immunodeficiency virus, J. Mol. Biol. 331 (2003) 213–229.

[25] A.S. Perelson, A.U. Neumann, M. Markowitz, J.M. Leonard, D.D. Ho, HIV-1 dynamics in vivo: virion clearance rate, infected cell life-span, and viral generation time, Science 271 (1996) 1582–1586.

[26] D.D. Ho, Perspectives series: host/pathogen interactions. Dynamics of HIV-1 replication in vivo, J. Clin. Invest. 99 (1997) 2565–2567.

[27] J. Suemitsu, M. Yoshida, N. Yamawaki, Y. Yamashita, Leukocytapheresis therapy by extracorporeal circulation using a leukocyte removal filter, Ther. Apher. 2 (1998) 31–36.

[28] H. Shibata, T. Kuriyama, N. Yamawaki, Cellsorba, Ther. Apher. Dial. 7 (2003) 44–47.

[29] J. Shirokaze, Leukocytapheresis using a leukocyte removal filter, Ther. Apher. 6 (2002) 261–266.

[30] K. Sugi, Filtration leukocytapheresis expected to ulcerative colitis treatment, Bio Clinica 12 (1997) 339–342.

[31] G. Pantaleo, C. Graziosi, J.F. Demarest, L. Butini, M. Montroni, C.H. Fox, J.M. Orenstein, D.P. Kotler, A.S. Fauci, HIV infection is active and progressive in lymphoid tissue during the clinically latent stage of disease, Nature 362 (1993) 355–358.

[32] L. Zhang, B. Ramratnam, K. Tenner-Racz, Y. He, M. Vesanen, S. Lewin, A. Talal, P. Racz, A.S. Perelson, B.T. Korber, M. Markowitz, Y. Guo, M. Duran, A. Hurley, J. Tsay, Y. Huang, C. Wang, D.D. Ho, Quantifying residual HIV-1 replication in patients receiving combination antiretroviral therapy, N. Engl. J. Med. 340 (1999) 1605–1613.

[33] J.M. Orenstein, C. Fox, S.M. Wahl, Macrophages as a source of HIV during opportunistic infections, Science 276 (1997) 1857–1861.

[34] A.T. Haase, K. Henry, M. Zupancic, G. Sedgewick, R.A. Faust, H. Melroe, W. Cavert, K. Gebhard, K. Staskus, Z. Zhang, P.J. Dailey, H.H. Balfour., A. Erice,

A.S. Perelson, Quantitative image analysis of HIV-1 infection in lymphoid tissue, Science 274 (1996) 985–988.

[35] D. Finzi, J. Blankson, J.D. Siliciano, J.B. Margolick, K. Chadwick, T. Pierson, K. Smith, J. Lisziewicz, F. Lori, C. Flexner, T.C. Quinn, R.E. Chaisson, E. Rosenberg, B. Walker, S. Gange, J. Gallant, R.F. Siliciano, Latent infection of CD4+ T cells provides a mechanism for lifelong persistence of HIV-1, even in patients on effective combination therapy, Nat. Med. 5 (1999) 512–517.

[36] M.A. Nowak, R. May, Virus Dynamics: Mathematical Principles of immunology and Virology, Oxford University Press, USA, 2000.

[37] A.S. Perelson, Modelling viral and immune system dynamics, Nat. Rev. Immunol. 2 (2002) 28–36.

[38] A.S. Perelson, P.W. Nelson, Mathematical analysis of HIV-I: dynamics in vivo, SIAM Rev. 41 (1999) 3–44.

[39] M.A. Stafford, L. Corey, Y. Cao, E.S. Daar, D.D. Ho, A.S. Perelson, Modeling plasma virus concentration during primary HIV infection, J. Theor. Biol. 203 (2000) 285–301.

[40] G. Pantaleo, C. Graziosi, L. Butini, P.A. Pizzo, S.M. Schnittman, D.P. Kotler, A.S. Fauci, Lymphoid organs function as major reservoirs for human immunodeficiency virus, Proc. Natl. Acad. Sci. USA 88 (1991) 9838–9842.

[41] O.J. Cohen, G. Pantaleo, G.K. Lam, A.S. Fauci, Studies on lymphoid tissue from HIV-infected individuals: implications for the design of therapeutic strategies, Springer Semin. Immunopathol. 18 (1997) 305–322.

[42] L.E. Hood, I.L. Weissmann, W.B. Wood, J.H. Wilson, Immunology, The Benjamin/Cummings Publishing Company, Menlo Park, CA, 1984.

[43] S. Wolfram, Statistical mechanics of cellular automata, Rev. Mod. Phys. 55 (1983) 601–644.

[44] S. Wolfram, Universality and complexity in cellular automata, Physica D 10 (1984) 1–35.

[45] R.M. Zorzenon dos Santos, S. Coutinho, Dynamics of HIV infection: A cellular automata approach, Phys. Rev. Lett. 87 (2001) 168102.

[46] V. Shi, A. Tridane, Y. Kuang, A viral load-based cellular automata approach to modeling HIV dynamics and drug treatment, J. Theor. Biol. 253 (2008) 24–35.

[47] E.G. Burkhead, J.M. Hawkins, D.K. Molinek, A dynamical study of a cellular automata model of the spread of HIV in a lymph node, Bull. Math. Biol. 71 (2009) 25–74.

[48] D.C. Douek, R.D. McFarland, P.H. Keiser, E.A. Gage, J.M. Massey, B.F. Haynes, M.A. Polis, A.T. Haase, M.B. Feinberg, J.L. Sullivan, B.D. Jamieson, J.A. Zack, L.J. Picker, R.A. Koup, Changes in thymic function with age and during the treatment of HIV infection, Nature 396 (1998) 690–695.

[49] G. Pantaleo, A.S. Fauci, Immunopathogenesis of HIV infection 1, Annu. Rev. Microbiol. 50 (1996) 825–854.

[50] J. Weber, The pathogenesis of HIV-1 infection, Br. Med. Bull. 58 (2001) 61–72.

[51] G. Pantaleo, C. Graziosi, J.F. Demarest, O.J. Cohen, M. Vaccarezza, K. Gantt, C. Muro-Cacho, A.S. Fauci, Role of lymphoid organs in the pathogenesis of human immunodeficiency virus (HIV) infection, Immunol. Rev. 140 (1994) 105–130.

[52] B. Tindall, D.A. Cooper, Primary HIV infection: host responses and intervention strategies, AIDS 5 (1991) 1–14.

[53] E.S. Daar, T. Moudgil, R.D. Mayer, D.D. Ho, Transient high levels of viremia in patients with primary human immunodeficiency virus type 1 infection, N. Engl. J. Med. 324 (1991) 961–964.

[54] P.O. Pehrson, S. Lindbäck, C. Lidman, H. Gaines, J. Giesecke, Longer survival after HIV infection for injecting drug users than for homosexual men: implications for immunology, AIDS 11 (1997) 1007–1012.

[55] P. Goulder, R.E. Phillips, R.A. Colbert, S. McAdam, G. Ogg, M.A. Nowak, P. Giangrande, G. Iuzzi, B. Morgan, A. Edwards, A.J. McMichael, S. Rowland-Jones, Late escape from an immunodominant cytotoxic T-lymphocyte response associated with progression to AIDS, Nat. Med 3 (1997) 212–217.

[56] P. Klenerman, S. Rowland-Jones, S. McAdam, J. Edwards, S. Daenke, D. Ialloo, B. Köppe, W. Rosenberg, D. Boyd, A. Edwards, P. Giangrande, R.E. Phillips, A.J. McMichael, Cytotoxic T-cell activity antagonized by naturally occurring HIV-1 Gag variants, Nature 369 (1994) 403–407.

[57] X. Wei, J.M. Decker, S. Wang, H. Hui, J.C. Kappes, X. Wu, J.F. Salazar-Gonzalez, M.G. Salazar, J.M. Kilby, M.S. Saag, N.L. Komarova, M.A. Nowak, B.H. Hahn, P.D. Kwong, G.M. Shaw, Antibody neutralization and escape by HIV-1, Nature 422 (2003) 307–312.

[58] B. Ramratnam, J.E. Mittler, L. Zhang, D. Boden, A. Hurley, F. Fang, C.A. Macken, A.S. Perelson, M. Markowitz, D.D. Ho, The decay of the latent reservoir of replication-competent HIV-1 is inversely correlated with the extent of residual viral replication during prolonged anti-retroviral therapy, Nat. Med. 6 (2000) 82–85.

[59] A. Pierratos, M. Ouwendyk, R. Francoeur, S. Vas, D.S. Raj, A.M. Ecclestone, V. Langos, R. Uldall, Nocturnal hemodialysis: three-year experience, J. Am. Soc. Nephrol. 9 (1998) 859–868.

[60] H. Schiffl, S.M. Lang, R. Fischer, Daily hemodialysis and the outcome of acute renal failure, N. Engl. J. Med. 346 (2002) 305–310.

[61] A.W. Williams, S.B. Chebrolu, T.S. Ing, G. Ting, C.R. Blagg, Z.J. Twardowski, Y. Woredekal, B. Delano, V.C. Gandhi, C.M. Kjellstrand, Early clinical, quality-of-life, and biochemical changes of "daily hemodialysis" (6 dialyses per week), Am. J. Kidney Dis. 43 (2004) 90–102.

[62] A. Pierratos, New approaches to hemodialysis, Annu. Rev. Med. 55 (2004) 179–189.

[63] R. Galland, J. Traeger, W. Arkouche, C. Cleaud, E. Delawari, D. Fouque, Short daily hemodialysis rapidly improves nutritional status in hemodialysis patients, Kidney Int. 60 (2001) 1555–1560.

[64] F. Locatelli, U. Buoncristiani, B. Canaud, H. Kohler, T. Petitclerc, P. Zucchelli, Dialysis dose and frequency, Nephrol. Dial. Transplant 20 (2005) 285–296.
[65] C.R. Blagg, C.M. Kjellstrand, G.O. Ting, B.A. Young, Comparison of survival between short-daily hemodialysis and conventional hemodialysis using the standardized mortality ratio, Hemodial. Int. 10 (2006) 371–374.

**Monamorn Precharattana** was born in Bangkok, Thailand, in1984. She received a B.Sc. degree from Physics Department, Kasetsart University, Bangkok, Thailand, in 2006. Now she is a Ph.D. candidate in Physics Department, in Mahidol University. Her research interests focus on biophysics and simulations.

**Artorn Nokkaew** was born in Bangkok, Thailand, in 1982. He received a B.Sc. in Computer science from Udon Thani Rajabhat University, Thailand, in 2005. He is now a Ph.D. candidate in Science and Technology Education at Mahidol University, Thailand. His research interests focus on modeling & application in Mathematics education.

**Wannapong Triampo** was born in Nakhonratchasima Province, Thailand, in 1970. He received a Ph.D. in Physics from Virginia Tech, USA, in 2001. After graduation, he has been with Mahidol University, Thailand, where he is now an Associate Professor in Physics. His research interests focus on biophysics and stochastic modeling.

**Darapond Triampo** was born in Bangkok, Thailand, in 1973. She received a Ph.D. in Chemical, Biomedical Materials Engineering from Stevens Institute, USA, in 2000. After graduation, she has been with Mahidol University, Thailand, where she is now a lecturer in Chemistry. Her research interests focus on studying of the interaction between materials and biological systems.

**Yongwimon Lenbury** was born in Bangkok, Thailand, in1952. She received a Ph.D. in Mathematics from Vanderbilt University. After graduation, she has been with Mahidol University, Thailand, where she is a Professor in Mathematics. Her research interests focus on applied mathematics and modeling.